

# Modulation of a High-Current Relativistic Electron Beam in a Low-Density Background Plasma

J.D. Miller, R.F. Schneider, D.J. Weidman<sup>(a)</sup>, and H.S. Uhm  
 Naval Surface Warfare Center, Silver Spring, MD 20903-5000

and

K.T. Nguyen  
 Mission Research Corporation, Newington, VA 22122

## Abstract

Modulation of the beam current has been observed during ion focused regime (IFR) transport of a high-power relativistic electron beam propagating through a low-density background plasma. In this experiment, a 1.7-MeV, 1-kA, risetime-sharpened electron beam is transported in a KrF excimer laser produced IFR channel in TMA gas. The IFR channel is immersed in a low-density plasma filled transport tube. We present experimental measurements and computer simulations demonstrating modulation of this high-current relativistic electron beam near the low-density background plasma frequency.

## Introduction

Plasma wakefields are well known in the high-energy physics community. The plasma wakefield accelerator (PWFA)<sup>1</sup> utilizes the longitudinal electric fields in plasma waves excited by a short duration bunched relativistic electron beam as a source of high accelerating gradients. In the PWFA, intense electron bunches are utilized as a driver beam to excite wakefields in a high density plasma. These wakefields are then used to accelerate a low-current trailing beam.<sup>2,3</sup> The work reported here involves experimental measurements on high-current (kA level) relativistic electron beams whose transport is strongly influenced by self-induced wakefields.

A high-current relativistic electron beam injected into a preionized plasma channel causes channel electrons to be expelled by the electrostatic force generated by the head of the beam and permits stable electron beam transport.<sup>4-8</sup> If the plasma channel is immersed in a low-density background plasma, both channel electrons and plasma electrons inside the charge neutralization radius are ejected by the beam head, provided the combined channel and background plasma density is less than the beam density. The charge neutralization radius is the point at which the total enclosed channel and background plasma ion charge is equal to the beam charge. The charge neutralization radius is given by

$$r_n = r_b \sqrt{\left[ \left( \frac{r_c}{r_b} \right)^2 + \frac{(1 - (r_c / r_b)^2) f_e}{g} \right]}$$

where  $r_b$  is the beam radius,  $r_c$  is the channel radius,  $f_e = n_c/n_b$  is the space charge neutralization fraction and is the ratio of the channel ion density to the electron beam density, and  $g = n_p/n_b$  is the ratio of the ion density outside the channel to the electron beam density. The background electrons beyond the charge neutralization radius are not expelled, but they are perturbed by the beam head and begin to oscillate at a frequency near that of the electron plasma frequency of the low-density background plasma,  $\omega_p = (n_p e^2 / \epsilon_0 m_e)^{1/2}$ . These radial plasma oscillations produce an electrostatic wakefield with electric field components in the radial and axial directions. The longitudinal component of this field, traveling with the beam, causes

accelerating and decelerating forces on beam electrons leading to beam energy and current modulation. These effects were first observed for high-current beams in computer simulations<sup>9</sup> and were seen to lead to eventual beam disruption. Most of what is known about this beam-plasma interaction is due to analytical calculations<sup>10,11</sup> and numerical simulations<sup>9-11</sup> with no direct experimental measurements.

## Experimental Setup

In the experiment, a 1.7-MeV, 6-kA, 30-ns electron beam produced by a Febetron 705 is passed through a beam risetime sharpener and matched onto a laser produced IFR channel in trimethylamine (TMA) gas. Figure 1 is a schematic diagram of the experiment. The electron beam is generated from a 2.5-cm-diam velvet cathode and is extracted into a beam risetime sharpening cell through a 6  $\mu$ m aluminized mylar anode foil. The risetime sharpener cell<sup>12</sup> uses a single magnetic lens to preferentially focus the high energy portion of the beam at an aperture. This results in a 1-kA electron beam, with a 5-ns risetime and a 13-ns flattop, exiting the risetime sharpening cell through a second aluminized mylar foil in front of the 3-cm-diam graphite aperture plate. The beam extracted through this aperture is matched onto a KrF excimer laser ionized IFR channel.

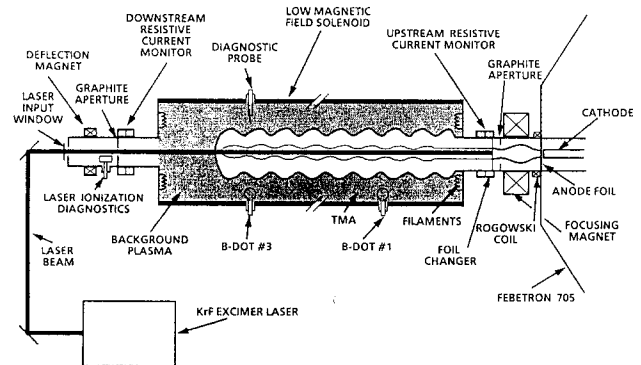


Figure 1 Schematic of the plasma wakefield experiment.

The 3-cm-diam laser ionized channel is formed by two-step photoionization of TMA using a 750-mJ, 248-nm, 30-ns KrF excimer laser. The TMA gas flows through the transport chamber continuously to provide a stable gas pressure in the range 0.2 - 0.8 mTorr. These TMA pressures result in space-charge neutralization fractions sufficient to efficiently propagate the electron beam in the absence of a background plasma. The beam risetime sharpener cell and the diode region are maintained at a lower pressure, on the order of  $10^{-5}$  Torr, to prevent diode shorting or gas focusing effects. The TMA pressure is measured with ionization gauges calibrated to a Baratron capacitance manometer. The laser is fired to ionize the TMA typically 500 ns before the voltage is applied to the diode.

# Report Documentation Page

*Form Approved*  
*OMB No. 0704-0188*

Public reporting burden for the collection of information is estimated to average 1 hour per response, including the time for reviewing instructions, searching existing data sources, gathering and maintaining the data needed, and completing and reviewing the collection of information. Send comments regarding this burden estimate or any other aspect of this collection of information, including suggestions for reducing this burden, to Washington Headquarters Services, Directorate for Information Operations and Reports, 1215 Jefferson Davis Highway, Suite 1204, Arlington VA 22202-4302. Respondents should be aware that notwithstanding any other provision of law, no person shall be subject to a penalty for failing to comply with a collection of information if it does not display a currently valid OMB control number.

1. REPORT DATE <b>JUN 1991</b>	2. REPORT TYPE <b>N/A</b>	3. DATES COVERED <b>-</b>			
4. TITLE AND SUBTITLE <b>Modulation of a High-Current Relativistic Electron Beam in a Low-Density Background Plasma</b>		5a. CONTRACT NUMBER			
		5b. GRANT NUMBER			
		5c. PROGRAM ELEMENT NUMBER			
6. AUTHOR(S)		5d. PROJECT NUMBER			
		5e. TASK NUMBER			
		5f. WORK UNIT NUMBER			
7. PERFORMING ORGANIZATION NAME(S) AND ADDRESS(ES) <b>Naval Surface Warfare Center, Silver Spring, MD 2b903-5000</b>		8. PERFORMING ORGANIZATION REPORT NUMBER			
9. SPONSORING/MONITORING AGENCY NAME(S) AND ADDRESS(ES)		10. SPONSOR/MONITOR'S ACRONYM(S)			
		11. SPONSOR/MONITOR'S REPORT NUMBER(S)			
12. DISTRIBUTION/AVAILABILITY STATEMENT <b>Approved for public release, distribution unlimited</b>					
13. SUPPLEMENTARY NOTES <b>See also ADM002371. 2013 IEEE Pulsed Power Conference, Digest of Technical Papers 1976-2013, and Abstracts of the 2013 IEEE International Conference on Plasma Science. Held in San Francisco, CA on 16-21 June 2013. U.S. Government or Federal Purpose Rights License</b>					
14. ABSTRACT <b>Modulation of the beam current has been observed during ion focused regime (IFR) transport of a high-power relativistic electron beam propagating through a low-density background plasma. In this experiment, a 1.7-MeV, 1-kA, risetime-sharpened electron beam is transported in a KrF excimer laser produced IFR channel in TMA gas. The IFR channel is immersed in a low-density plasma filled transport tube. We present experimental measurements and computer simulations demonstrating modulation of this high-current relativistic electron beam near the low-density background plasma frequency.</b>					
15. SUBJECT TERMS					
16. SECURITY CLASSIFICATION OF:			17. LIMITATION OF ABSTRACT	18. NUMBER OF PAGES	19a. NAME OF RESPONSIBLE PERSON
a. REPORT <b>unclassified</b>	b. ABSTRACT <b>unclassified</b>	c. THIS PAGE <b>unclassified</b>	<b>SAR</b>	<b>4</b>	

The laser produced channel is centered in a 0.5-m-diam, 3.6-m-long plasma filled transport chamber. The low-density background plasma filling the transport chamber is generated by a hot filament discharge in the low pressure TMA gas. The discharge is pulsed for durations less than 1-ms to reduce the level of TMA fragmentation before the laser is fired.<sup>13</sup> The gas pressure is sufficiently low that beam-induced ionization of the TMA is negligible. Plasma characteristics measured by Langmuir<sup>14</sup> and microwave resonator<sup>15</sup> probe techniques indicate that the plasma has good uniformity axially, radially, and azimuthally.<sup>16</sup> A low axial magnetic field (on the order of 5 G) is present for plasma confinement and to improve the uniformity. This field is sufficiently small so as not to influence the electron beam dynamics. The plasma density is adjustable in the range  $10^8$  to  $5 \times 10^9$  cm<sup>-3</sup>.

The beam current is monitored prior to injection into the plasma filled transport chamber and after exiting the chamber by resistive wall current monitors.<sup>17</sup> Uncalibrated, single-turn B-dot loops located axially along the transport chamber monitor the evolution of the modulation of the current. It should be noted that both monitors are sensitive to the net current flowing in the transport chamber. A scintillator-photodiode observed the x-ray signal emitted when the beam electrons were deflected to the wall at the end of the transport chamber to avoid striking the laser input window.

### Experimental Results

Initial experimental measurements have demonstrated very well defined current oscillations impressed upon the electron beam after traversing the 3.6-m-long transport chamber. These oscillations are in the range 150 to 300 MHz and are very close to the electron plasma frequency of the low density background plasma. In the absence of the background plasma, the most efficient electron beam transport occurred for a space-charge neutralization fraction of  $f_e \approx 0.9$  as determined by the laser channel ionization measurements. This is indicative of a fairly high transverse beam temperature and is common to electron beams generated and propagated using these techniques.

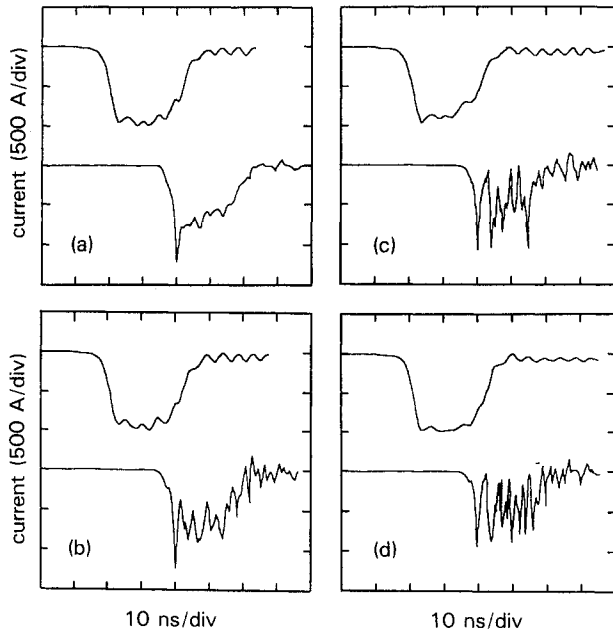


**Figure 2** Current waveforms from the resistive wall current monitors; (a)  $n_p=0$ , (b)  $n_p=1.0 \times 10^9$  cm<sup>-3</sup>, (c)  $n_p=1.5 \times 10^9$  cm<sup>-3</sup>, (d)  $n_p=2.0 \times 10^9$  cm<sup>-3</sup>. Top (bottom) waveform: current entering (exiting) the transport chamber.

The evolution of the current oscillations is characterized in the typical waveforms shown in Fig. 2. Figure 2(a) shows the response of the resistive wall current monitors in the absence of the background plasma. The currents are shown prior to the entrance of the beam into the transport chamber (upper waveform) and after exiting the chamber (lower waveform). Examination of the transported current waveform indicates a steepening of the current risetime with an associated spike at the front end of the pulse. This is due to a combination of inductive beam erosion and the fact that the beam voltage pulse is nearly sinusoidal and varies throughout the current pulse.<sup>18</sup> Figures 2(b)-(d) illustrate the development of current oscillations with increasing background plasma density. The plasma densities have been inferred from dc biased (+40 V) Langmuir probe data without any correction for finite sheath effects. The space charge neutralization fraction at the peak beam current for all the data presented here was  $f_e \approx 0.9$ , giving a neutralization radius,  $r_n$ , ranging from 3.0 cm (Fig. 2(b)) to 2.4 cm (Fig. 2(d)). For these experimental parameters,  $g$  assumes values in the range  $0 \leq g \leq 0.06$ , indicating that the low density background plasma does not contribute significantly to the space charge neutralization fraction of the channel. The data in Figs. 2(c) and (d) indicate that the current becomes severely modulated after only 3.6 m of transport in the plasma background. Increasing the plasma density higher than that shown in Fig. 2(d) resulted in loss of transport efficiency and eventual beam disruption as indicated by the current monitors and the x-ray signal picked up by the scintillator-photodiode.

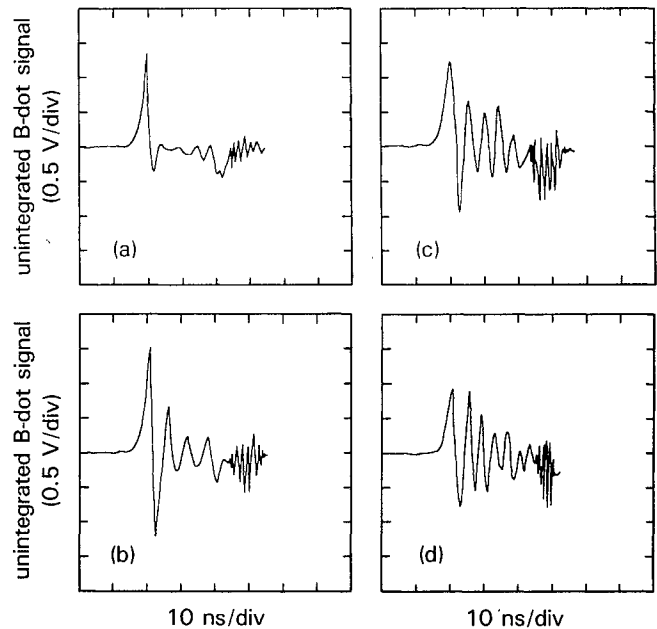


**Figure 3** Unintegrated B-dot loop response 0.9 m downstream from the entrance to the plasma filled transport chamber; (a)  $n_p=0$ , (b)  $n_p=6.3 \times 10^8$  cm<sup>-3</sup>, (c)  $n_p=1.0 \times 10^9$  cm<sup>-3</sup>, (d)  $n_p=1.5 \times 10^9$  cm<sup>-3</sup>.

The frequency of oscillation is more readily determined from the unintegrated B-dot loop data. Figure 3 shows the unintegrated B-dot loop response from the probe located 0.9 m downstream from the entrance to the plasma-filled transport chamber. The current oscillations are quite clear and indicate an increasing frequency with increasing plasma density. The dependence of the background plasma density on the oscillation frequency obtained from the unintegrated B-dot loop data is shown in Fig. 4. The solid line represents a least squares fit of the data to a  $n_p^{1/2}$  dependence. This functional dependence indicates that the experimentally observed current oscillation frequency scales quite well with the low density background electron plasma frequency.

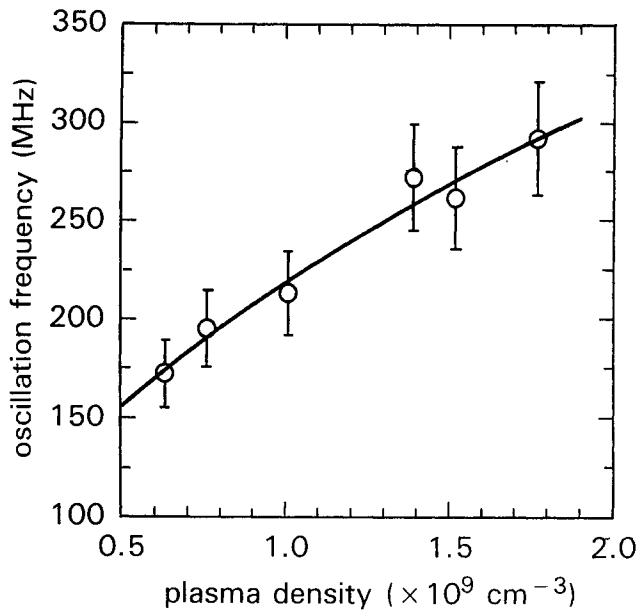


**Figure 4** Oscillation frequency from the unintegrated B-dot loop data as a function of the background plasma density.

#### Computer Simulations

Numerical simulations have also been performed to predict the behavior of the electron beam in the plasma filled chamber using the fully electromagnetic 2-1/2 dimensional particle-in-cell code MAGIC.<sup>19</sup> The beam and channel properties in the simulation correspond quite closely to the experimental conditions described previously. The transport chamber was filled with a uniform diffuse plasma at a density of  $2 \times 10^9 \text{ cm}^{-3}$ . The evolution of the electron beam current in the transport chamber at different axial locations is

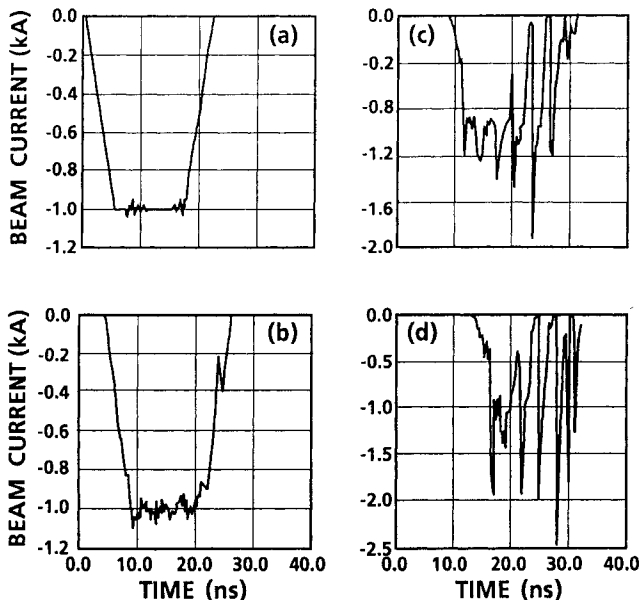


**Figure 5** Beam current waveforms from the MAGIC simulation at (a)  $z=0 \text{ m}$ , (b)  $z=1.1 \text{ m}$ , (c)  $z=2.3 \text{ m}$ , and (d)  $z=3.4 \text{ m}$  downstream from the entrance to the plasma filled transport chamber for  $n_p = 2.0 \times 10^9 \text{ cm}^{-3}$ .

shown in Fig. 5(a)-(d). The beam current profile in Fig. 5(a) corresponds to the experimentally measured electron beam current prior to injection to the plasma filled chamber and the simulation waveform in Fig. 5(d) to the experimentally measured waveform upon exiting the chamber. The simulation clearly shows the ability of the diffuse plasma to strongly modulate the beam current. This result compares very well to the experimental data shown in Fig. 2.

Figure 6 illustrates the modulation of the electron beam power by the low-density background plasma. The input beam power shown in Fig. 6(a) is approximately triangular in shape with a peak near the midpoint of the pulse of approximately 1.75 GW. After traversing the 3.6 m long plasma chamber however, the output beam power pulse is modulated at a frequency of about 350 MHz, very near the background plasma frequency of 400 MHz for this simulation. As a result, the instantaneous peak power has reached levels in excess of 2.6 GW.

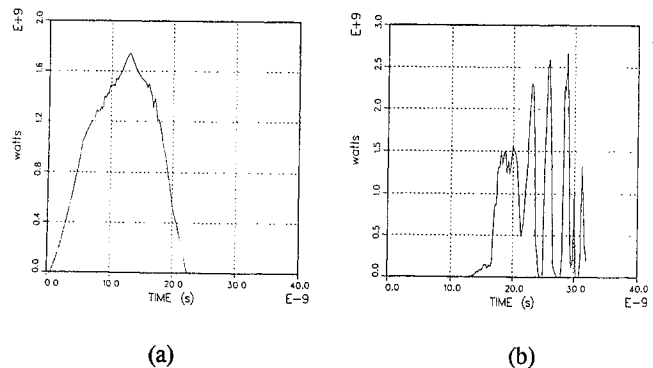


**Figure 6** Electron beam power (a) injected into the plasma-filled transport tube, and (b) after 3.4 m of propagation in the plasma-filled transport tube.

#### Summary

We have observed very well-defined current oscillations impressed upon a high-current relativistic electron beam propagating in an IFR channel immersed in a low-density background plasma. Severe effects on beam current transport have been observed for  $g$  parameter values in the range 0.03 to 0.06 after only 3.6 m of beam transport. Initial results indicate the frequency of current oscillation to be near the plasma frequency of the low-density background plasma, consistent with the predictions of plasma wakefield theory and simulation.

The authors would like to thank J. Goldhar and W.C. Freeman for technical assistance, and G. Joyce for helpful discussions. This work was supported by the Strategic Defence Initiative Organization under funding document number N0001490WX15505 and Independent Research funds at the Naval Surface Warfare Center.

<sup>(a)</sup> permanent address: Advanced Technology and Research, Laurel, MD 20707

<sup>1</sup> P. Chen, J.M. Dawson, R.W. Huff, and T. Katsouleas, Phys. Rev. Lett. **54**, 693 (1985).

<sup>2</sup> J.B. Rosenzweig, P. Schoessow, B. Cole, W. Gai, R. Konecny, J. Norem, and J. Simpson, Phys. Rev. A **39**, 1586 (1989).

<sup>3</sup> J.B. Rosenzweig, D.B. Cline, B. Cole, H. Figueroa, W. Gai, R. Konecny, J. Norem, P. Schoessow, and J. Simpson, Phys. Rev. Lett. **61**, 98 (1988).

- <sup>4</sup> W.E. Martin, G.J. Caporaso, W.M. Fawley, D. Prosnitz, and A.G. Cole, *Phys. Rev. Lett.* **54**, 685 (1985); G.J. Caporaso, F. Rainer, W.E. Martin, D.S. Prono, and A.G. Cole, *Phys. Rev. Lett.* **57**, 1591 (1986)
- <sup>5</sup> R.L. Carlson, S.W. Downey, and D.C. Moir, *J. Appl. Phys.* **61**, 12 (1986).
- <sup>6</sup> C.A. Frost, S.L. Shope, R.B. Miller, G.T. Leifeste, C.E. Crist, and W.W. Reinstra, *IEEE Trans. Nucl. Sci.* **NS-32**, 2754 (1985).
- <sup>7</sup> H.L. Buchanan, *Phys. Fluids* **30**, 231 (1987).
- <sup>8</sup> S.L. Shope, C.A. Frost, G.T. Leifeste, and J.W. Poukey, *Phys. Rev. Lett.* **58**, 531 (1987).
- <sup>9</sup> M.A. Mostrom and B.S. Newberger, *Bull. Am. Phys. Soc.* **31**, 1399 (1986).
- <sup>10</sup> H.S. Uhm, *Phys. Lett. A* **149**, 469 (1990).
- <sup>11</sup> H.S. Uhm and G. Joyce, accepted for publication in *Phys. Fluids B*.
- <sup>12</sup> J.D. Miller, R.F. Schneider, H.S. Uhm, K.T. Nguyen, K.W. Struve, and D.J. Weidman, Naval Surface Warfare Center Technical Report, NAVSWC TR 90-268, 1990, unpublished; J.D. Miller, K.T. Nguyen, R.F. Schneider, K.W. Struve, H.S. Uhm, and D.J. Weidman, Proceedings of the XIVth International Symposium on Discharges and Electrical Insulation in Vacuum, Santa Fe, N.M., Sept. 17-20, 1990, p. 730.
- <sup>13</sup> J.D. Miller, R.F. Schneider, and J. Goldhar, Naval Surface Warfare Center Technical Note, NAVSWC TN 90-326, 1990, unpublished.
- <sup>14</sup> F.F. Chen, in *Plasma Diagnostics Techniques*, R.H. Huddleston and S.L. Leonard, eds., (Academic Press, New York, 1965), p. 113.
- <sup>15</sup> R.L. Stenzel, *Rev. Sci. Instrum.* **47**, 603 (1976).
- <sup>16</sup> J.D. Miller, R.F. Schneider, H.S. Uhm, and D.J. Weidman, Naval Surface Warfare Center Technical Note, NAVSWC TN 90-428, 1990, unpublished; H.S. Uhm, J.D. Miller, R.F. Schneider, and D.J. Weidman, accepted for publication in *IEEE Trans. Plasma Sci.*
- <sup>17</sup> K.W. Struve, Conference Record of the Workshop on Measurements of Electrical Quantities in Pulse Power Systems II, (IEEE Catalog No. 86CH2327-5, 1988), p. 36.
- <sup>18</sup> J.R. Smith (private communication).
- <sup>19</sup> B. Goplen, L. Ludeking, J. McDonald, G. Warren, and R. Worl, Mission Research Corporation Report No. MRC/WDC-R-216, 1989, unpublished.